UV Resonance Raman Excitation Profile through the $^1B_{2u}$ State of Benzene

Sanford A. Asher* and Craig R. Johnson

Department of Chemistry, University of Pittsburgh, Pittsburgh, Pennsylvania 15260
(Received: October 12, 1984)

The dispersion of the total differential Raman cross section of the 992-cm^{-1} a_{1g} benzene ring breathing vibration has been measured between 600 and 217 nm. The Raman intensity with visible and near-UV excitation is dominated by states in the far-UV. Excitation profile data between 217 and 250 nm indicate that the main source of Raman intensity derives from the $^1E_{1u}$ and, possibly, the $^1B_{1u}$ excited states. A small contribution of the $^1B_{2u}$ state is observed through oscillations in the Raman intensity due to the interference phenomena previously predicted by Korenowski et al. (*J. Chem. Phys.* **1978**, *68*, 1248). Enhancement of overtones is observed with excitation below ca. 230 nm.

The utility of resonance Raman spectroscopy as a sensitive and selective probe of molecular structure for chromophoric species in complex matrices has been extensively documented over the past decade.[1] Numerous results have appeared on heme protein structure,[2-5] visual pigments,[4,5] and nucleic acid structure.[6-8] Other studies have used resonance Raman spectroscopy to examine excited-state geometries and to assign electronic transitions.[6-10] With few exceptions[6-20] previous resonance Raman studies have been limited to molecules with chromophores absorbing in the visible spectral region. This has resulted from the lack of laser sources capable of exciting within the UV spectral region.[21]

We have recently constructed a novel UV resonance Raman spectrometer continously tunable between 217 and 800 nm[22] and have embarked on a program to demonstrate the sensitivity and selectivity available from UV resonance Raman studies of species absorbing in the UV spectral region. Our studies,[15-18,22] as well as those of others,[9,10,19] have demonstrated that the intense UV Raman spectra observed can be used to study aromatic molecules in complex samples, such as polycyclic aromatic hydrocarbons in coal liquids[15,16,18] and aromatic amino acids in proteins.[17,19] In this study we characterize the UV resonance Raman excitation profile of the symmetric ring stretching vibration (ν_1) of benzene. Any fundamental understanding of UV resonance Raman enhancement mechanisms in larger aromatics requires the elucidation of the resonance enhancement mechanism in benzene. This simple molecule has been extensively studied and a wealth of information is available on its electronic and vibrational states.[23,24]

Significant theoretical and experimental efforts have already been expended in Raman studies of benzene. A recent series of pioneering studies of benzene by Ziegler and Albrecht[11-14] utilizing preresonance Raman excitation came to the surprising conclusion that for preresonance excitation at wavelengths longer than 270 nm no Raman enhancement is evident from the lowest energy allowed transition to the $^1E_{1u}$ excited state at 183 nm or from the $^1B_{1u}$ or $^1B_{2u}$ excited states at 205 and 260 nm, respectively. The important state or states contributing to Raman intensity appear to occur in the far-UV at ca. 120 nm.[11,14] Further, they extrapolated their preresonance Raman experimental data in a theoretical study and predicted that large interference phenomena would occur for the 992-cm^{-1} ν_1 a_{1g} ring breathing vibration upon excitation into the vibronic bands of the $^1B_{2u}$ transition of benzene in the 230-260-nm spectral region. More recent studies[9,10] with 212.8-nm excitation which is almost resonant with the $^1B_{1u}$ transition of benzene and the ^1L_a transition of alkyl-substituted benzenes have shown that, as predicted by theory, overtones and combinations of e_{2g} vibrations are enhanced, almost exclusively, with excitation in this dipole forbidden transition.

We have directly measured the Raman excitation profile and the Raman cross sections of the ν_1 symmetric ring breathing vibration in the region between 217 and 600 nm and conclude that (1) the $^1E_{1u}$ state and possibly the $^1B_{1u}$ state are the major states contributing to Raman intensity for excitation between 220 and 250 nm; and (2) the $^1B_{2u}$ state shows only a small contribution to the UV resonance Raman intensities and its contribution is observed only very close to resonance. We observe the $^1B_{2u}$ interference phenomena previously predicted by Korenoswki et al.[14]

Experimental Section

Benzene and acetonitrile were used as supplied from Burdick and Jackson. The solution Raman spectra were measured in a closed cycle recirculating jet stream. The solution was pumped through a dye laser jet nozzle having a rectangular orifice of ca. 0.2 × 3 mm. Excitation of the sample by the laser occurred along the height of the jet and light was collected at 90°. The short (ca. 0.1 mm) path length for the 90° scattered light minimized self-absorption. The Raman spectrometer used has been described in detail elsewhere.[22] The excitation source is a Quanta Ray DCR-2A Nd:YAG Laser operated at 20 Hz and frequency doubled to pump a PDL dye laser. UV light was generated either by doubling the dye laser light or by mixing the doubled light with the 1.06-μm fundamental of the YAG laser in a Quanta Ray WEX harmonic generation crystal assembly.

The output of the WEX was used to excite the sample. Reflective optics including an ellipsoidal mirror were used to collect the scattered light in order to avoid chromatic aberrations. The

(1) Clark, R. J. H.; Stewart, B. *Struct. Bonding (Berlin)* **1979**, *36*, 1.
(2) Asher, S. A. *Methods Enzymol.* **1981**, *76*, 371.
(3) Spiro, T. G. In "Iron Porphyrins", Part II, Lever, A. B. P., Grey, H. B., Ed.; Addison-Wesley: Reading, MA, 1983.
(4) Carey, P. R. "Biochemical Applications of Raman and Resonance Raman Spectroscopies"; Academic Press: New York, 1982.
(5) Tu, A. T. "Raman Spectroscopy in Biology: Principles and Applications"; Wiley: New York, 1982.
(6) Peticolas, W. L.; Blazej, D. C. *Chem. Phys. Lett.* **1979**, *63*, 604.
(7) Suzubi, E.; Homoguchi, H.; Horoda, I.; Matsuura, H.; Shimanouchi, R. *J. Raman Spectrosc.* **1976**, *4*, 91.
(8) Laigle, A.; Chinsky, L.; Turpin, P.-Y. *Nucleic Acid Res.* **1982**, *10*, 1707.
(9) Ziegler, L. D.; Hudson, B. *J. Chem. Phys.* **1981**, *74*, 982.
(10) Ziegler, L. D.; Hudson, B. *J. Chem. Phys.* **1983**, *79*, 1134.
(11) Ziegler, L. D.; Albrecht, A. C. *J. Chem. Phys.* **1977**, *67*, 2753.
(12) Ziegler, L. D.; Albrecht, A. C. *J. Chem. Phys.* **1979**, *70*, 2634, 2644.
(13) Ziegler, L. D.; Albrecht, A. C. *J. Raman Spectrosc.* **1979**, *8*, 73.
(14) Korenowski, G. M.; Ziegler, L. D.; Albrecht, A. C. *J. Chem. Phys.* **1978**, *68*, 1248.
(15) Asher, S. A. *Anal. Chem.* **1984**, *56*, 720.
(16) Asher, S. A.; Johnson, C. R. *Science* **1984**, *225*, 311.
(17) Johnson, C. R.; Ludwig, M.; O'Donnell, S. E.; Asher, S. A. *J. Am. Chem. Soc.* **1984**, *106*, 5008.
(18) Johnson, C. R.; Asher, S. A. *Anal. Chem.* **1984**, *56*, 2258.
(19) Rava, R. P.; Spiro, T. G. *J. Am. Chem. Soc.* **1984**, *106*, 4062.
(20) Hong, H.-K.; Jacobsen, C. W. *J. Chem. Phys.* **1978**, *68*, 1170.
(21) Asher, S. A. *Appl. Spectrosc.* **1984**, *38*, 276.
(22) Asher, S. A.; Johnson, C. R.; Murtaugh, J. *Rev. Sci. Instrum.* **1983**, *54*, 1657.
(23) See for example: Robin, M. B. "Higher Excited States of Polyatomic Molecules"; Academic Press: New York, 1975; Vol. II.
(24) Ziegler, L. D.; Hudson, B. S. "Excited States", Lim, E. C., Ed.; Academic Press: New York, 1982; Vol. V, p 41.

0022-3654/85/2089-1375$01.50/0 © 1985 American Chemical Society

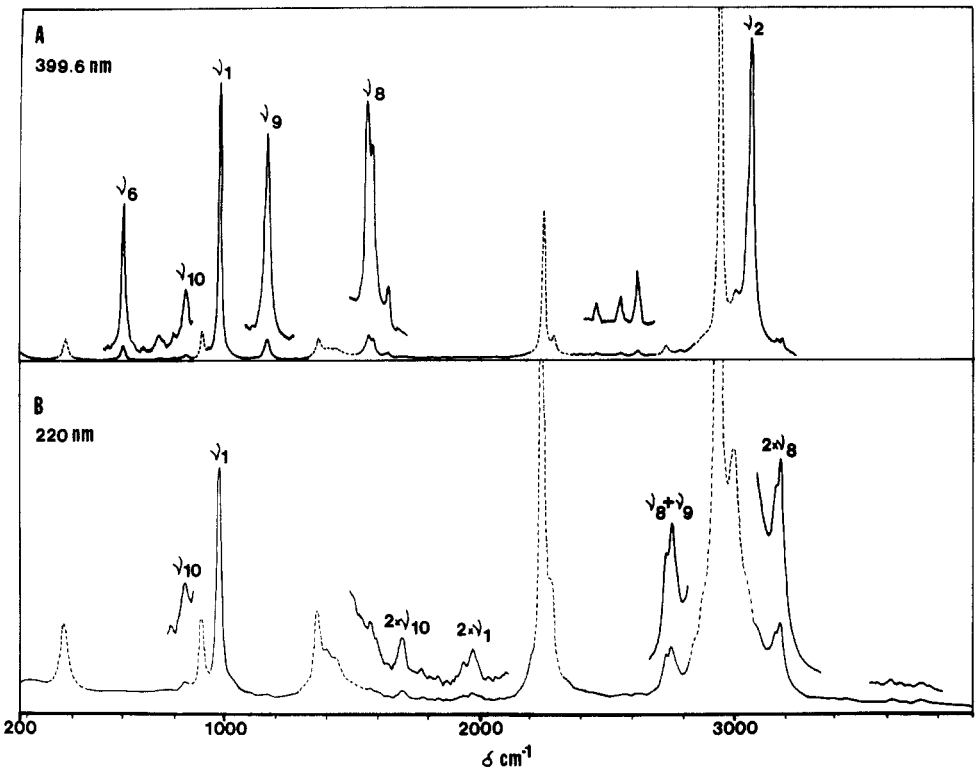

Figure 1. (A) Resonance Raman spectrum of a 40% by volume solution of benzene in acetonitrile excited at 399.6 nm. Band-pass ≃ 3 Å. Laser pulse energy = 3.5 mJ. Number of pulses averaged = 8416 (7 min scan). (B) Resonance Raman spectrum of a 1% by volume solution of benzene in acetonitrile excited at 220 nm. Band-pass ≃ 3 Å. Laser pulse energy = 0.5 mJ. Number of pulses averaged = 24000 (20 min scan).

polarization of the scattered light was randomized by a crystalline quartz wedge to avoid intensity artifacts deriving from any polarization efficiency bias of the monochromator gratings. The light was dispersed by using a modified Spex Triplemate monochromator. The scattered light was detected by using a PAR OMA II system which utilized a PAR 1420 blue-enhanced intensified Reticon detector. To minimize fluorescence interference the Reticon was gated on for 10-ns intervals which bracketed the 4-ns laser pulses. Depolarization ratios were measured with a Polacoat analyzer placed between the sample and the ellipsoidal collection mirror. The Polacoat analyzer was calibrated by measuring the transmission of the polarized Rayleigh scattering from the sample.

The throughput efficiency of the monochromator in the UV was calibrated by using a standard intensity deuterium lamp either imaged directly through the optical system or scattered from a Lambert surface prepared with Kodak white reflectance standard; however, because the internal standard Raman peak of acetonitrile was within 80 cm^{-1} of the 992-cm^{-1} benzene line no correction was necessary for either self-absorption or optical throughout bias when comparing the Raman intensity of the 992-cm^{-1} benzene line to the 918-cm^{-1} acetonitrile line. The excitation profile data derive from peak height measurements. We compared peak height measurements to peak area measurements over a limited region of the excitation profile and found almost perfect agreement.

We recently determined the dispersion of the Raman cross sections of the 918-cm^{-1} peak of CH_3CN and other molecules useful as internal intensity standards[25] (SO_4^{2-}, ClO_4^-, and NO_3^-). These results were used to correct our relative benzene excitation profile data for the dispersion of the Raman intensity of the 918-cm^{-1} CH_3CN stretching vibration. We determined the excitation profile of the total differential Raman cross section of benzene by indexing our 514.5-nm relative excitation profile data to an absolute total differential Raman cross section of 28.6 × 10^{-30} cm^2 sr^{-1} $molecule^{-1}$ measured for benzene by Abe et al.[26] However, because this benzene Raman cross section is for pure liquid benzene, and our data is for 1% benzene in acetonitrile (which has a refractive index of 1.361 at 514.5 nm), we used the local field correction[25,27] to obtain the relevant benzene Raman cross section of 19.2 × 10^{-30} cm^2 at 514.5 nm for our sample solution.

Absorption spectra of the solutions were measured before and after the Raman spectral measurements to ensure that no concentration changes occurred and that photochemical decomposition was absent. We defocused the excitation beam on the sample to avoid nonlinear Raman phenomena. The Raman intensity was found to increase in proportion to the incident intensity for each of the excitation wavelengths checked.

Results

Figure 1a shows the resonance Raman spectrum of a solution of 40% benzene in acetonitrile (by volume) excited at 399.6 nm. The acetonitrile peaks are indicated by the dashed line while the solid line corresponds to the benzene peaks. The benzene vibrational modes are labeled by using the Wilson convention with the ν_2 (3073 cm^{-1}) and ν_1 (992 cm^{-1}) bands corresponding to the two a_{1g} vibrations. The ν_2 and ν_1 bands derive from C–H stretching and carbon ring breathing, respectively. These are the Raman peaks showing the largest intensity when exciting in the visible and near-UV spectral region.

Figure 1B shows the resonance Raman spectrum of benzene excited at 220 nm and demonstrates the presence of numerous overtone and combination bands. This spectrum is qualitatively similar to those obtained recently for benzene and substituted derivatives by Ziegler and Hudson using 212-nm excitation.[9,10] However, the spectrum obtained with 220-nm excitation shows a larger intensity of the 992-cm^{-1} peak compared to the intensity of the overtones than was observed with 212-nm excitation.

Figure 2 shows a limited portion of the resonance Raman spectra of a 1% solution of benzene in acetonitrile excited at different wavelengths within the $^1B_{2u}$ absorption band. As the excitation wavelength decreases, the intensity of the 992-cm^{-1} benzene peak, labeled B, increases almost monotonically relative to the 918-cm^{-1} acetonitrile peak, labeled A. The poor signal-

(25) Dudik, J. M.; Johnson, C. R.; Asher, S. A. *J. Chem. Phys.*, in press.
(26) Abe, N.; Wakayama, M.; Ito, M. *J. Raman Spectrosc.* **1977**, *6*, 38.
(27) Schrotter, H. W.; Klochner, H. W. "Topics in Current Physics", Weber, A. Ed.; Springer-Verlag: Berlin, 1979; p 123.

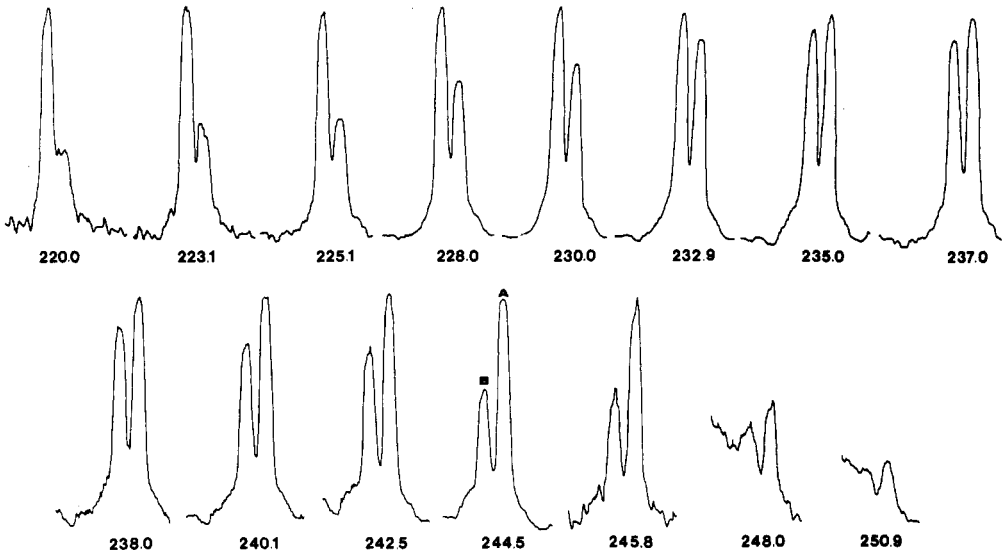

Figure 2. Resonance Raman spectra of a 1% by volume solution of benzene in acetonitrile at various excitation wavelengths. The bands marked B correspond to the 992-cm^{-1} benzene ν_1 vibration, while the bands marked A are from the acetonitrile 918-cm^{-1} vibration.

to-noise ratios of the spectra excited at 250.9 and 248.0 nm derive from benzene fluorescence interference.

The only *fundamental* benzene vibration to show a large relative intensity increase as excitation is tuned toward shorter wavelength is the 992-cm^{-1} peak. The relative intensities of the *overtone* vibrations also increase as the excitation wavelength decreases. However, the presence of the overtone peaks only becomes clearly evident in the spectra with excitation below ca. 230 nm.

We measured the depolarization ratio for the ν_1 vibration of benzene and found it to increase as the excitation wavelength decreased. The measured depolarization ratios for 90° scattering were $\rho_l = 0.01 \pm 0.01$, 0.04 ± 0.02, 0.04 ± 0.02, and 0.10 ± 0.02 at 560, 290, 230, and 220 nm, respectively.

Discussion

Figure 3 shows the absorption spectrum of benzene and the excitation profile data from Figure 2 as well as other data obtained with excitation at longer wavelengths. The insidious gap in the excitation profile between 37 000 and 40 000 cm^{-1} is due to benzene fluorescence interference. The excitation profile data in Figure 3A are plotted as the observed intensity of the 992-cm^{-1} benzene peak divided by that of the 918-cm^{-1} acetonitrile peak, but corrected for the dispersion of the 918-cm^{-1} acetonitrile Raman intensity.[25] The data in Figure 3A are linearly proportional to the square of the orientationally averaged Raman polarizability. Figure 3B shows the excitation frequency dependence of the total differential Raman cross section for benzene obtained for a 90° scattering geometry where both polarizations of the Raman scattered light are collected.

The excitation profiles in Figure 3 show that as the excitation energy increases from 18 000 to 38 000 cm^{-1} the magnitude of the square of the Raman polarizability and the Raman cross section of the benzene 992-cm^{-1} band slowly increases. The rate of increase accelerates rapidly for excitation energies above 40 000 cm^{-1}. However, it should be noted that the two segments of the excitation profile, above 40 000 and below 37 000 cm^{-1}, cannot be smoothly connected; the values for the 992-cm^{-1} peak are higher at 37 000 than at 40 000 cm^{-1}.

The Raman excitation profile data can be understood by considering the factors important for Raman intensity. The total Raman scattering cross section, σ_{mn}, for the Raman vibrational transition $n \leftarrow m$ over 4π sr for an isolated molecule averaged over all orientations is[27-29]

$$\sigma_{mn} = \frac{I_{mn}}{I_0} = \frac{2^7\pi^5}{3^2}\nu_0(\nu_0 - \nu_{mn})^3 G f(T) \sum_{\rho\sigma} |\alpha_{\rho\sigma}(\nu_0)|^2 \qquad (1)$$

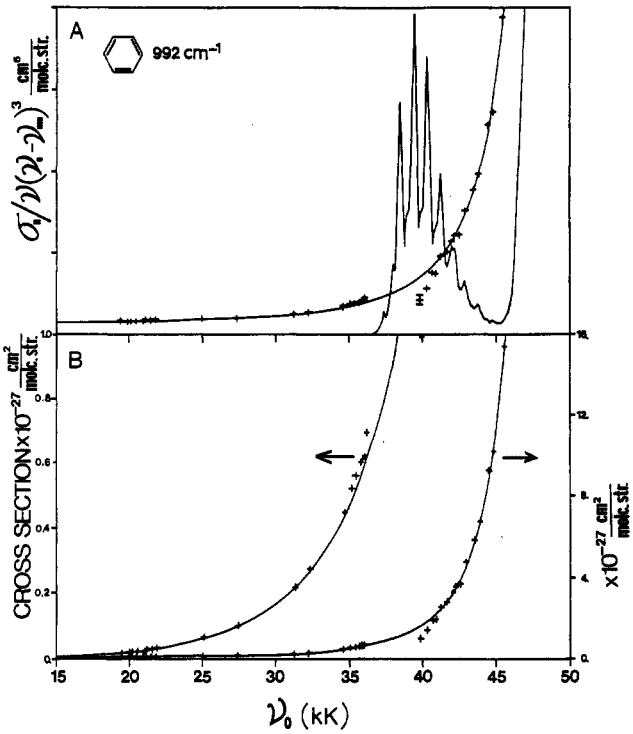

Figure 3. Absorption spectrum of benzene in the UV and the resonance Raman excitation profile. (A) The excitation profile data are displayed as the ratio of the peak height intensity of the 992-cm^{-1} benzene peak to that of the 918-cm^{-1} acetonitrile peak normalized to the Raman intensity dispersion of CH_3CN (see text). The crosses label measured points in the excitation profile while the line corresponds to a nonlinear least-squares best fit to eq 5. The error bars indicating a 95% confidence level are shown for the worst excitation profile datum. (B) Total differential Raman cross section of benzene. The lower frequency data are expanded by a factor of 16 for easier visualization and are indexed by the oridinate scale on the left.

I_{mn} is the integrated Raman scattered intensity (photon/(s cm^2)) over 4π sr integrated over the bandwidth of the vibrational transition $n \leftarrow m$. I_0 and ν_0 are the incident excitation beam intensity and frequency (cm^{-1}) while ν_{mn} corresponds to the frequency of the Raman vibrational mode (cm^{-1}). G is a factor specifying the degeneracy of the initial state, m, while $f(T)$ is the Boltzmann weighting factor specifying the thermal occupancy of

(28) Eckhardt, G.; Wagner, W. G. *J. Mol. Spectrosc.* **1977**, *6*, 38.

(29) See for example: Tang, J.; Albrecht, A. C. in "Raman Spectroscopy, Theory and Practice", Szymanski, H. A., Ed.; Plenum Press: New York, 1970; Vol. II, p 33.

the initial state. The factor $\nu_0(\nu_0 - \nu_{mn})^3$ appears rather than $(\nu_0 - \nu_{mn})^4$ (as is commonly seen) because the intensities are defined in units of photon/(s cm^2) for photon counting detection. $\alpha_{\rho\sigma}(\nu_0)$ is the ρ,σth ($\rho,\sigma = x,yz$) component of the Raman polarizability tensor averaged over all molecular orientations for the excitation frequency, ν_0.

For 90° Raman scattering measurements from a solution where the incident light is polarized perpendicular to the scattering plane, and both the parallel and perpendicular scattering polarization are collected, the total differential Raman scattering cross section, σ_R, is given by[27-32]

$$\sigma_R = \frac{d\sigma_{mn}(\nu_0)}{d\Omega} = \frac{2^4\pi^4}{45} b^2 G \frac{L\nu_0(\nu_0 - \nu_{mn})^3}{1 - \exp(-hc\nu_{mn}/kT)}(45\alpha^2 + 7\gamma^2 + 5\delta^2) \quad (2)$$

where b is the zero point vibrational amplitude

$$b = (h/8\pi c^2 \nu_{mn})^{1/2}$$

and α^2, γ^2, and δ^2 are the isotropic, anisotropic, and antisymmetric[32] invariants of the polarizability tensor, respectively, and h, c, k, and T and Planck's constant, the speed of light, Boltzmann's constant, and the temperature, respectively. L is the local field correction for the condensed phase sample and specifies the increased electric field amplitude in the sample over that which would be present in the gas phase.[25-27]

The components of the polarizability tensor, $\sigma_{\rho\sigma}$, are given by second-order perturbation theory as[29,30]

$$\alpha_{\rho\sigma} = \sum_{ev}\left[\frac{\langle gm|R_\sigma|ev\rangle\langle ev|R_\rho|gn\rangle}{\nu_{ev} - \nu_m - \nu_0 + i\Gamma_e} + \frac{\langle gm|R_\rho|ev\rangle\langle ev|R_\sigma|gn\rangle}{\nu_{ev} - \nu_n + \nu_0 + i\Gamma_e}\right] \quad (3)$$

where ρ and σ are molecular coordinates which label the components of the polarizability tensor. R_σ is the electric dipole moment operator along the molecular coordinate, σ. ν_{ev} is the transition frequency corresponding to an excited vibrational level of an excited electronic state, e. Γ_e is the damping factor associated with the excited state, e, and ν_m and ν_n are the frequencies associated with the vibrational levels m and n in the ground electronic state. The summation in eq 2 is over all molecular excited states ev except for the ground state. The Raman transition occurs between vibrational levels m and n of the ground electronic state, g.

This expression predicts that the Raman intensity will increase as resonance is approached. In normal Raman scattering numerous electronic transitions contribute to the Raman intensity. However, the contribution of each transition is weighted by the magnitude of the transition moments in the numerator as well as the energy terms in the denominator; given similar transition moments, the electronic transition closest to the excitation frequency should contribute most.

The Raman excitation profile and the Raman depolarization ratios for the 992-cm^{-1} benzene vibration indicate that the low-energy transitions (to the in-plane polarized $^1B_{2u}$, $^1B_{1u}$, and $^1E_{2u}$ states) do not dominate the Raman intensities observed with visible and near-UV excitation. This is evident from the low value[31] of the depolarization ratio ($\rho_1 = 0.02$), which indicates a relatively isotropic Raman tensor.

$$\rho_1 = \frac{3\gamma^2 + 5\delta^2}{45\alpha^2 + 4\gamma^2}$$

For the symmetric ν_1 vibration of benzene, $\alpha_{\rho\sigma} = \alpha_{\sigma\rho}$, and $\delta^2 = 0$. Thus

$$\rho_1 = \frac{3\gamma^2}{45\alpha^2 + 4\gamma^2}$$

where

$$\alpha = \tfrac{1}{3}(\alpha_{xx} + \alpha_{yy} + \alpha_{zz})$$

$$\gamma^2 = \tfrac{1}{2}\{(\alpha_{xx} - \alpha_{yy})^2 + (\alpha_{yy} - \alpha_{zz})^2 + (\alpha_{zz} - \alpha_{xx})^2 + \tfrac{3}{2}[(\alpha_{xy} + \alpha_{yx})^2 + (\alpha_{yx} + \alpha_{xy})^2 + (\alpha_{zx} + \alpha_{xz})^2]\}$$

$$\delta^2 = \tfrac{3}{4}\{(\alpha_{xy} - \alpha_{yx})^2 + (\alpha_{yz} - \alpha_{zy})^2 + (\alpha_{zx} - \alpha_{xz})^2\}$$

α^2, γ^2, and δ^2 are the isotropic, anisotropic, and antisymmetric invariants of the Raman polarizability.[32]

If the subscripts x, y, and z correspond to the principal axes of the polarizability ellipsoid for benzene

$$\gamma^2 = \tfrac{1}{2}\{(\alpha_{xx} - \alpha_{yy})^2 + (\alpha_{yy} - \alpha_{zz})^2 + (\alpha_{zz} - \alpha_{xx})^2\}$$

The x and y axes are in the plane of the ring while the z axis is perpendicular to the ring. If the in-plane polarized transitions dominate the Raman scattering $\alpha_{xx} = \alpha_{yy}$, $\alpha_{zz} = 0$, and ρ_1 should be equal to 0.125. In constrast, the measured $\rho_1 = 0.02$ indicates that the magnitude of α_{zz} is similar to α_{xx}, α_{yy}. Two solutions for the ratio α_{zz}/α_{xx} exist for $\rho_1 = 0.02$. Either $\alpha_{zz}/\alpha_{xx} = 0.53$ or 1.68. This indicates that either the magnitude of the z component of the polarizability α_{zz} is ca. half that of α_{xx}, α_{yy}, or a factor 50% greater than α_{xx}, α_{yy}. (It should be noted that a similar analysis by Korenowski et al.[14] resulted in slightly different values for the ratios but similar conclusions. The difference presumably arises because Korenoswki et al. interpreted the published depolarization ratio[31] to be ρ_n, the depolarization ratio for naturally polarized light.)

The fact that the $^1B_{2u}$, $^1B_{1u}$, and $^1E_{1u}$ excited states do not dominate the visible wavelength Raman intensities was known earlier from the preresonance Raman excitation profile study[11] of benzene using excitation energies below 35 000 cm^{-1}. Using the Albrecht A term preresonance approximation[29,33] to eq 3

$$\frac{\sigma_R}{\nu_0(\nu_0 - \nu_{mn})^3} = K\left[\frac{\nu_e^2 + \nu_0^2}{(\nu_e^2 - \nu_0^2)^2}\right]^2 \quad (4)$$

Ziegler and Albrecht found that the observed preresonance Raman intensities could be accounted for by a single UV transition localized at ca. 81 000 cm^{-1} (124 nm). K is a scaling constant and ν_e is the resonant excited-state frequency. In agreement with this earlier excitation profile study a similar analysis of our preresonance excitation profile data results in a far-UV transition centered at ca. 84 000 cm^{-1} (119 nm). Presumably, this calculated state represents some weighted average of the numerous transitions occurring in the far-UV spectral region. Similar far-UV resonant state enhancements derive from Albrecht A term modeling of the UV preresonance Raman excitation profiles of the C–C and C≡N stretches of CH_3CN,[25] the C–C and C=O stretches of acetone,[34] the vibrations of N-methylacetamide,[34] and the symmetric stretching vibrations[25] of SO_4^{2-} and ClO_4^-.

The selection of a far-UV excited state by the A term indicates that none of the longer wavelength transitions dominate the preresonance Raman intensities. This could occur because of cancellations between the contributions of different excited states to the Raman polarizability; the different states could contribute with opposite sign. The preresonance Raman intensities excited at wavelengths longer than 280 nm show no contribution from the $^1E_{1u}$ or $^1B_{1u}$ transitions at 183 and 205 nm.

As excitation approaches the transition to the $^1B_{2u}$ state from lower energy the Raman intensity begins to increase. The contribution of the $^1B_{2u}$ state clearly appears in the excitation profile through a decreased Raman intensity upon excitation between 40 000 and 42 000 cm^{-1}. This deenhancement which derives from destructive interferences between the higher-energy transition and vibronic components of the transition to the $^1B_{2u}$ state is qualitatively similar to that predicted for the $^1B_{2u}$ state earlier by Korenowski et al.[14] Indeed, we also appear to detect the inter-

(30) Albrecht, A. C. J. Chem. Phys. 1961, 34, 1476.
(31) Skinner, J. G.; Nilsen, W. G. J. Opt. Soc. Am. 1968, 58, 113.
(32) Long, D. A. "Raman Spectroscopy"; McGraw-Hill: New York, 1977.
(33) Albrecht, A. C.; Hutley, M. C. J. Chem. Phys. 1971, 55, 4438.
(34) Dudik, J. M.; Johnson, C. R.; Asher, S. A. J. Phys. Chem., in press.

ference oscillations of the Raman intensity about the individual vibronic components of the $^1B_{2u}$ absorption band predicted by Korenowski et al.[14]

We have carefully evaluated the statistical variance of our experimental data and the possible systematic errors such as throughput efficiency bias and self-absorption errors. For the worst case, at 40 000 cm^{-1} the relative standard deviation of the measurements is less than 10%. For more typical data it is less than 4%. This suggests that the oscillations of the excitation profile data at 42 000 and 43 000 cm^{-1} may be real and result from interference between vibronic components of the transition to the $^1B_{2u}$ state and the preresonant contribution of states higher energy.

The Raman polarizability increases sharply with excitation above 40 000 cm^{-1}. To estimate the transition energy of the state or states which contribute to the rapidly increasing Raman polarizability between 43 000 and 46 000 cm^{-1} we fit the excitation profile data to a modified form of the Albrecht A term (eq 4). The expression we use is

$$\frac{\sigma_R}{\nu_0(\nu_0 - \nu_{mn})^3} = \left(K_1 \frac{\nu_e^2 + \nu_0^2}{(\nu_e^2 - \nu_0^2)^2} + K_2 \right)^2 \qquad (5)$$

where K_2 is a constant which phenomenologically acts as a preresonant state at very high energy which makes an almost frequency-independent contribution to the Raman intensity; however, because it adds at the amplitude level to the Raman intensity, the cross terms give a small frequency-dependent contribution.

The solid curves in Figure 3 correspond to a least-squares best fit to the Raman data collected between 15 000 and 36 000 and 43 000 and 46 000 cm^{-1}. The data between 36 000 and 43 000 cm^{-1} were not used in the fit because these data show a contribution of the $^1B_{2u}$ state which is not included in eq 5. The fit which successfully models the excitation profile results in a transition energy of 52 500 cm^{-1} (191 nm) for the resonant state. This energy is close to that of the first dipole allowed electronic transition in benzene; the transition to the E_{1u} state has its absorption maximum at 54 500 cm^{-1} (183 nm) in n-heptane.[35] With 400-nm excitation, at the amplitude level, the second term, K_2, dominates the Raman polarizability by contributing essentially 2.6 times that of the preresonance term. In contrast at 230 nm (220 nm) the preresonance term is 3.2 (5.2) times K_2. Thus, the Raman intensity in the UV is dominated by states close to 190 nm.

The Raman cross sections were obtained by multiplying the data from Figure 3A by $\nu_0(\nu_0 - \nu_{mn})^3$ and scaling the result to the measured benzene cross section at 514.4 nm. Except in the region around the $^1B_{2u}$ absorption band the total differential benzene Raman cross section, σ_R in units of $cm^2/(molecule\ sr)$, can be obtained from the expression

$$\sigma_R(\nu_0) = K_3\nu_0(\nu_0 - 992)^3\left(\frac{\nu_e^2 + \nu_0^2}{(\nu_e^2 - \nu_0^2)^2} + K_2' \right)^2 \qquad (6)$$

where K_3 is 2.55×10^{-29} $cm^4/(molecule\ sr)$, ν_0 is in cm^{-1}, and K_2' is 1.975×10^{-9} cm^2. The solid line in Figure 3B shows the variation of the benzene cross section obtained by using eq 6 and the listed parameters. The benzene cross section increases from 19.2×10^{-30} $cm^2/(molecule\ sr)$ at 514.5-nm excitation to 15.2×10^{-27} $cm^2/(molecule\ sr)$ at 220 nm.

ρ_l also increases as the excitation energy increases. At 45 455-cm^{-1} excitation (220 nm) $\rho_l = 0.10 \pm 0.02$ which indicates that the ratio of the out-of-plane to the in-plane contribution to the Raman tensor α_{zz}/α_{xx} is 0.09 ± 0.07, or 3.3 ± 0.5. Either the in-plane electronic transitions dominate by a factor of ca. 20 or z-polarized transitions contribute a factor of 1.5 more than the in-plane transitions. The transition energy calculated from the data indicates that the main contribution to the preresonant enhancement below 250-nm excitation results from a transition or transitions to a state or states close to 191 nm which must be the in-plane polarized $^1E_{1u}$ and/or $^1B_{1u}$ states at 183 and 205 nm, respectively. Thus, the true α_{zz}/α_{xx} is probably 0.09 ± 0.07.

Assuming Albrecht A term enhancements, one finds that the $^1B_{1u}$ and $^1E_{1u}$ states should both contribute almost equally to the Raman intensities for excitation in the region between 213 and 220 nm; although the oscillator strength of the $^1E_{1u}$ transition is almost a factor of ten greater than that of the $^1B_{1u}$ transition,[35] the closer proximity of the $^1B_{1u}$ transition to the excitation frequency results in similar contributions from the $^1B_{1u}$ and $^1E_{1u}$ transitions. It should be noted that we assume the $^1B_{1u}$ transition shows an A termlike enhancement with a transition energy at the false origin associated with the vibronically active mode. To experimentally resolve the $^1E_{1u}$ and $^1B_{1u}$ state contributions will require additional Raman studies with excitation further into resonance with the $^1E_{1u}$ and $^1B_{1u}$ states.

Conclusions

The Raman intensity of the ν_1 a_{1g} 992-cm^{-1} benzene vibration in the visible and near-UV spectral regions derives mainly from states in the far-UV. The major source of intensity for excitation in the UV above 40 000 cm^{-1} derives from a state or states close to 190 nm which are x,y polarized and presumably are the $^1E_{1u}$ and $^1B_{1u}$ transitions. Only a small contribution to the Raman intensity derives from the dipole forbidden $^1B_{2u}$ state. Previously predicted $^1B_{2u}$ interference phenomena are observed. We have measured the total differential Raman cross section for the ν_1 symmetric stretch of benzene from 600 to 217 nm.

Acknowledgment. We gratefully acknowledge Professor Gerald Korenowski for helpful comments and Colleen Jones and Thanh Phung for technical help in these studies. We also gratefully acknowledge support for this study from NSF instrumentation Grant PCM-8115738 and NIH Grant 1R01 GM 30741-03. Acknowledgment is also made to the donors of the Petroleum Research Fund, administered by the American Chemical Society. We also acknowledge starter grant support from a Cottrell Research Corporation Grant and BRSG Grant 2S07 RR 07084-016 awarded by the Biomedical Research Support Grant Program, Division of Research Resources, National Institutes of Health. We also acknowledge support from an American Cancer Society Institutional Grant provided to the University of Pittsburgh. S. A. Asher is an Established Investigator of the American Heart Association.

Registry No. Benzene, 71-43-2.

(35) Robin, M. B. "Higher Excited State of Polyatomic Molecules"; Academic Press: New York, 1975, Vol. II, pp 210–223.